



Universidad Autónoma  
de Madrid

**Biblos-e Archivo**  
Repositorio Institucional UAM

Repositorio Institucional de la Universidad Autónoma de Madrid

<https://repositorio.uam.es>

Esta es la **versión de autor** del artículo publicado en:

This is an **author produced version** of a paper published in:

Applied Catalysis B: Environmental 96.1-2 (2010):148-156

**DOI:** <https://doi.org/10.1016/j.apcatb.2010.02.012>

**Copyright:** © 2010 Elsevier Ltd. This manuscript version is made available under the CC-BY-NC-ND 4.0 licence <http://creativecommons.org/licenses/by-nc-nd/4.0/>

El acceso a la versión del editor puede requerir la suscripción del recurso

Access to the published version may require subscription

# **Hydrodechlorination of chloromethanes with Pd on activated carbon catalysts for the treatment of residual gas streams**

M.A. Álvarez-Montero, L.M. Gómez-Sainero\*, M. Martín-Martínez, F. Heras and J.J. Rodríguez

Área de Ingeniería Química, Facultad de Ciencias, Universidad Autónoma de Madrid,  
Cantoblanco, 28049 Madrid, Spain.

**\* To whom correspondence should be addressed:** [luisa.gomez@uam.es](mailto:luisa.gomez@uam.es)

## Abstract

With a view of application in the treatment of residual gaseous streams contaminated by chloromethanes, the gas-phase HDC of chloroform (CLF), dichloromethane (DCM) and monochloromethane (MCM) with Pd on activated carbon catalysts has been investigated. Several catalysts were prepared using  $\text{PdCl}_2$  and  $\text{Pd}(\text{NO}_3)_2$  as the precursors and activated carbon with different particle size within the range of 0.25 to 2.8 mm. Catalytic experiments were performed in a fixed bed reactor at atmospheric pressure, using a molar ratio  $\text{H}_2/\text{chloromethane} = 100$ , chloromethane concentration in the inlet gas of 1000 ppm, space-times in the range of  $\tau = 0.08\text{--}1.73$   $\text{kg.h.mol}^{-1}$  and temperatures of 150–250 °C. Reactivity follows the order  $\text{CLF} > \text{DCM} > \text{MCM}$ . High selectivities to non-chlorinated products were obtained (> than 90% in most cases). Selectivity to methane decreases as the chlorine content of the molecule increases, in benefit of  $\text{C}_2\text{--C}_4$  hydrocarbons. The analysis of the evolution of yield and selectivities to reaction products with space-time in the HDC of chloroform suggests that all are primary products. Methane, monochloromethane and dichloromethane would be formed from the hydrogenation of the corresponding adsorbed chloride radical, while condensation products proceed from the reaction of two or more adsorbed radicals. The catalyst undergoes significant deactivation in the HDC of MCM and DCM, specially for this second, whereas it shows much more stable in the case of CLF. Characterization results suggest that deactivation of the catalyst in the HDC of DCM is due to a great decrease of the accessible metal surface which can be attributed to the poisoning of the active centres with reactants and reaction products. The use of  $\text{Pd}(\text{NO}_3)_2$  as Pd precursor instead of  $\text{PdCl}_2$  leads to a decrease in the total activity and TOF of the catalysts as a consequence of its poorer Pd dispersion and a lower proportion of electrodeficient Pd species. The use of different carbon particle size in the preparation of the catalysts did not show a significant effect in the activity.

**Keywords:** hydrodechlorination, residual gases, dichloromethane, chloroform, monochloromethane, Pd/activated carbon catalysts

## INTRODUCTION

Chlorinated volatile organic compounds play an important role in the chemical and pharmaceutical industry, where they are used as solvents and reactants. They are also employed in aerosols, adhesives, dry cleaning, etc [1]. However, because of its high toxicity and carcinogenic character these compounds are classified nowadays among the most important types of atmospheric pollutants [2,3]; chloroform and dichloromethane are included in the EPA's Toxic Release Inventory (TRI). Moreover, emission of organic chlorinated compounds to the atmosphere contributes to the destruction of the ozone layer, to the formation of photochemical smog and to global warming [2-4]. Emission of these compounds is restricted by strong legal regulations. This leads to the need of developing effective technologies for the treatment of residual streams contaminated with these pollutants. Catalytic hydrodechlorination (HDC) becomes, in this way, one of the most promising emerging technologies. This process has potential economic and environmental advantages over other methods, because it operates at low temperatures and atmospheric pressure and the reaction products are less hazardous than the ones resulting from other techniques [1,5-7].

There is a growing bibliography devoted to hydrodechlorination of organochlorinated compounds with catalysts based on different metals and supports. However, most of them are referred to the HDC of carbon tetrachloride (there are few references dealing with other chloromethanes) and mainly focused in the obtention of chloroform [8-13]. On the other hand, there is also scarce work focused on the hydrodechlorination of chloromethanes at low concentrations [14], which is the most common situation for residual gas effluents. In the work mentioned above [14], different catalysts based on Pd and Ni over several supports ( $\text{SiO}_2$ ,  $\text{TiO}_2$ ,  $\text{ZrO}_2$  and  $\text{Al}_2\text{O}_3$ ) and synthesized by different methods, cogellation and impregnation, were tested in the gas-phase hydrodechlorination of DCM at a concentration of 1200 ppm. Pd catalysts prepared by impregnation were more active and selective. Pd/ $\text{TiO}_2$  was the

most active, though this catalyst underwent a strong deactivation. On the other hand, Pd/SiO<sub>2</sub> catalyst showed moderate activity and more resistance to deactivation than other catalysts. However, acceptable activity was maintained for only 48h.

Other references including results in the deep gas-phase HDC of dichloromethane over different supported metallic catalysts can be found [15-17]. Mori et al. reported that Pd/SiO<sub>2</sub> showed high activity at 200 °C and atmospheric pressure. López et al. studied hydrodechlorination of several organochlorides (dichloromethane, tetrachloroethylene, chlorobenzene and 1,2-dichlorobenzene), all of them alone and in mixtures, over Pd/Al<sub>2</sub>O<sub>3</sub> catalyst. Dichloromethane conversions were lower than 30% in all the cases though selectivities toward non-chlorinated species were higher than 95%. Prati et al. tested different metals (Pd and Pt) in the hydrodechlorination of chloromethanes, the best results being obtained with Pd. Some other papers devoted to the HDC of chloroform and dichloromethane with precious metals catalysts (Pd/Al<sub>2</sub>O<sub>3</sub>, Pt/Al<sub>2</sub>O<sub>3</sub>, Rh/Al<sub>2</sub>O<sub>3</sub>, Pt/C, Pd/SiO<sub>2</sub>, etc) can be consulted in references [5,18,19]. However, all these works have been carried out in liquid-phase or at high concentrations, and none of them study the causes of catalyst deactivation which is a limiting issue regarding technological application.

In a previous work, gas-phase hydrodechlorination of dichloromethane with commercial and own-made Pd on activated carbon (Pd/C) catalysts was investigated [1], with very good results of activity and selectivity to non-chlorinated products, though the catalysts underwent important deactivation.

In this contribution, the activity, selectivity and stability of several own-made 1.0% (w/w) Pd/C catalysts, in the gas-phase hydrodechlorination of three chloromethanes, chloroform (CLF), dichloromethane (DCM) and methyl chloride (MCM) is investigated. The possible causes of catalyst deactivation are also analysed.

## 2. EXPERIMENTAL

### 2.1. Catalyst preparation

Five palladium-loaded catalysts supported on a commercial activated carbon were prepared by incipient wetness impregnation. Four of these catalysts were prepared using aqueous solutions of  $\text{H}_2\text{PdCl}_4$  (from anhydrous  $\text{PdCl}_2$  supplied by Sigma-Aldrich) of appropriate concentration to obtain 1 wt % Pd nominal load, varying the carbon particle size ( $d_p$ ) as follow: PdCCl-1 ( $d_p = 0.25\text{-}0.5$  mm), PdCCl-2 ( $d_p = 0.5\text{-}1.0$  mm), PdCCl-3 ( $d_p = 1.0\text{-}2.0$  mm) and PdCCl-4 ( $d_p = 2.0\text{-}2.8$  mm). In order to analyze the effect of the palladium precursor, another catalyst (PdCN) was prepared in the same way but using  $\text{Pd}(\text{NO}_3)_2$  (Fluka) as precursor of the active phase and a carbon particle size in the range of 0.25-0.5 mm. After drying, activation of all the catalysts was carried out by reduction under continuous  $\text{H}_2$  flow. The samples were heated up to 250 °C at a heating rate of 10 °C/min and maintained at this temperature for 2h. Hydrogen was supplied by Praxair with a minimum purity of 99.999 %.

### 2.2. Catalyst Characterization

The porous structure of the catalysts was characterized from the 77 K  $\text{N}_2$  adsorption-desorption isotherms using a Quantachrome Autosorb 6B apparatus. The samples were previously outgassed during 4 h at 250 °C and a residual pressure of  $10^{-3}$  torr.

The bulk palladium content was determined via inductive coupled plasma-mass spectroscopy (ICP-MS) in a Perkin-Elmer model Elan 6000 Sciex system that was equipped with an autosampler (Perkin-Elmer model AS-91). The samples were previously digested for 15 min in a microwave oven, using a strongly acid mixture at 180 °C.

The X-Ray Diffraction patterns of the catalysts and supports were obtained in a X'Pert PRO Panalytical Diffractometer. The powdered sample was scanned using Cu K $\alpha$  monochromatic radiation ( $\lambda = 0.15406$  nm) and a Ge Mono filter. A scanning range of  $2\theta = 10$  to  $100^\circ$  and scan step size of  $0.020^\circ$  with 5 s collection time were used.

The surface of the catalysts was analyzed by X-ray photoelectron spectroscopy (XPS) with a Physical Electronics 5700C Multitechnique System, using Mg K $\alpha$  radiation ( $h\nu = 1253.6$  eV). To determine all the elements present in the catalyst surface, general spectra were recorded for the samples, by scanning up to a binding energy (BE) of 1200 eV. The BE of the Pd  $3d_{5/2}$  core level and full width at half maximum (FWHM) values were used to determine the chemical state of Pd. Correction for binding energies due to sample charging were done by taking the C 1s peak (284.6 eV) as an internal standard. The accuracy of the BE scale was  $\pm 0.1$  eV. The data analysis procedure involved smoothing, a Shirley background subtraction and curve fitting using mixed Gaussian-Lorentzian functions by a least-squares method. Atomic ratios of the elements were calculated from the relative peak areas of the respective core level lines using Wagner sensitivity factors [20].

A Micromeritics ChemiSorb 2705 pulse analyzer was used to measure the accessibility of surface sites by CO chemisorption at room temperature. The sample (0.15-0.30 g) was first reduced at  $250^\circ\text{C}$  for 2h under hydrogen flow and then cooled under helium flow at room temperature. Several pulses of 50  $\mu\text{L}$  CO were then introduced until saturation of the catalyst surface was achieved. The number of exposed palladium atoms ( $\text{Pd}_s$ ) was calculated from CO chemisorption data ( $\text{CO}_{\text{ads}}$ ). The stoichiometry of the adsorption of CO over palladium atoms ( $\text{Pd}_s/\text{CO}_{\text{ads}}$ ) was assumed to be 1[21,22,23,24].

The number of Pd atoms accessible to the reactants in the analyzed sample is given by:

$$Pd_s = N_A \cdot CO_{ads} / CO_{ads}^M \quad (1)$$

where  $CO_{ads}$  is the volume of CO chemisorbed,  $CO_{ads}^M$  is the molar volume of CO, and  $N_A$  is Avogadro's number. The percentage dispersion of Pd,  $D$ , was calculated from the number of exposed,  $Pd_s$ , and total,  $Pd_t$ , Pd atoms from:

$$D (\%) = 100 \cdot Pd_s / Pd_t \quad (2)$$

### 2.3. Catalytic activity experiments

The activity of the catalysts in the hydrodechlorination of the chloromethanes was evaluated in a continuous flow reaction system described elsewhere [1], consisting essentially of a 9.5 mm i.d. fixed bed micro-reactor, coupled to a gas chromatograph with a FID detector for the analysis of the reaction products.

Experiments were performed at atmospheric pressure using a total flow rate of 100 Ncm<sup>3</sup>/min, and a H<sub>2</sub>/chloromethane molar ratio of 100. The gas feed, with a chloromethane concentration of 1000 ppm, was prepared by mixing adequate proportions of the starting chloromethane/N<sub>2</sub> commercial mixture and N<sub>2</sub>. The catalyst weight and temperature were adjusted to the desired values in each run. Space-times in the range of  $\tau = 0.08$ -1.73 kg.h.mol<sup>-1</sup> and temperatures of 150-250 °C were tested. Catalytic behaviour results are expressed in terms of chloromethane conversion ( $X_A$ ), selectivities to different reaction products ( $S_i$ ) and turnover frequency (TOF). The evolution of the catalytic activity, relative to the time on stream, was followed.

Reaction parameters were calculated as follows:



$$X_A(\%) = \frac{F_{A,in} - F_{A,out}}{F_{A,in}} \cdot 100$$

$$r_A = \frac{F_{A,in} \cdot X_A}{m_{Pd}}$$

$$S_i(\%) = \frac{n \cdot F_i}{F_{A,in} - F_{A,out}} \cdot 100$$

$$TOF = \frac{r_A \cdot 106.4}{D} \cdot 100$$

where  $F_{A,in}$  and  $F_{A,out}$  are the chloromethane molar flow rates at the inlet and at the outlet of the reactor, respectively,  $r_A$  is the rate of the chloromethane transformation,  $m_{Pd}$  the mass of palladium loaded,  $D$  the Pd dispersion (%) and  $n$  the stoichiometric coefficient of product  $i$  in the HDC reaction .

### 3. RESULTS AND DISCUSSION

#### 3.1 Characterization of the catalysts

Table 1 summarizes the BET surface area, pore volume, bulk Pd content and the Pd dispersion values of all the fresh catalysts. For one of them (PdCCl-1) results after being used in the hydrodechlorination of dichloromethane are also included.

The 77 K N<sub>2</sub> adsorption-desorption isotherms of the catalysts approached to Type I of the BDDT classification, being indicative of microporous solids, although a contribution of mesopores is also present in some extent. All of them show a high BET surface area, with values well above 1200 m<sup>2</sup>/g, even for the used catalyst, indicating that constriction or partial blockage of the porous structure do not occur upon reaction, at the relative mild temperatures used in the experiments. Nor the different particle size of the carbon used as support, neither the use of a different precursor show any significant effect on the textural properties of the catalysts.

All the fresh catalysts show good Pd dispersion values, although a significant decrease (around 30%) is observed when using Pd nitrate as precursor, which some authors have attributed to the existence of a different type of adsorption sites [25]. Selecting a suitable Pd precursor appears to be decisive to obtain highly dispersed Pd catalysts. The use of acid solutions of Pd chloride leads to the formation of tetrachloropalladic acid which strongly interacts with the surface of carbon through the adsorption equilibrium  $\text{PdCl}_4^{2-} + \text{A} \leftrightarrow \text{PdCl}_{(4-n)}^{(2-n)-} \text{A} + n\text{Cl}^-$ . According to these authors, this leads to the formation of small Pd particles homogeneously distributed inside the pores of the catalyst with palladium at electrodeficient state. In contrast, when  $\text{Pd}(\text{NO}_3)_2$  is used as precursor, Pd is more weakly deposited and predominantly in the external surface. A scarce influence of the carbon particle size used for catalyst preparation (within the wide range explored) in the Pd dispersion can be observed, since it slightly but monotonically decreases as the carbon particle size increases. This effect was also found by Simonov et al. [25].

Figure 1 shows the XPS profiles of as prepared and reduced fresh PdCCl-1 catalyst, as well as after being used. In accordance with the results obtained in previous works [1,26], core level spectra of Pd 3d orbitals show the existence of mainly an oxidation state of Pd for the as prepared catalyst, and Pd species in two different oxidation states in the reduced sample. A main band centered at a binding energy of 337 eV was observed for Pd 3d<sub>5/2</sub> in the as prepared unreduced catalyst. Two main bands centered at binding energy values around 335.5 eV and 337 eV were observed for Pd 3d<sub>5/2</sub> in the reduced catalyst, which can be attributed to metallic palladium (Pd<sup>0</sup>) and electro-deficient palladium (Pd<sup>n+</sup>), respectively. Integration of the areas under the curves yields fairly similar relative proportions of these two species as it was found in previous works [1,26]. The use of the catalyst in the HDC reaction leads to a decrease in the proportion of the electrodeficient Pd species.

Figure 2 reports the Pd 3d XPS spectra of the fresh catalyst prepared from Pd nitrate (PdCN). Significant differences were found with the spectra of the PdCCl-1 catalyst. In the sample of PdCN prior to reduction, the presence of the two species of Pd, electrodeficient and reduced, can be observed. Core level spectra of Pd 3d<sub>5/2</sub> orbital shows two main bands centered at 337.19 eV and 335.3 eV respectively. This is an evidence of partial reduction of PdCN catalyst during the impregnation process, which leads to a lower Pd dispersion (Table 1) and is in agreement with the findings of different authors [25,26]. In consequence, the higher proportion of reduced species in the starting as prepared PdCN catalyst, in addition to the weaker interaction of Pd with the support, leads to a much higher proportion of Pd in reduced state in the final catalyst (once reduced in H<sub>2</sub> atmosphere), which highly affects to its activity, as it will be seen later.

Figure 3 shows the 3d XPS spectra of the catalysts prepared with different carbon particle size. As was seen for the PdCCl-1 catalyst, in the samples after impregnation and prior to reduction (Fig 3a) Pd is mainly in electrodeficient state, though the proportion of reduced Pd slightly increases as the carbon particle size increases. That could be the cause of the slight decrease in Pd dispersion observed in these catalysts when increasing the particle size of the activated carbon support (Table 1). After reduction, in the H<sub>2</sub> atmosphere, all the catalysts show significant amounts of both species, electrodeficient and reduced Pd, although still the proportion of the second is higher as the carbon particle size increases.

Figure 4 shows the XRD diffraction profiles of PdCCl-1 catalyst reduced and after used in the HDC of DCM. A peak at 2 $\theta$  value of 40° is observed in the fresh sample which corresponds to Pd particles in the cubic system. The pattern of the used catalyst shows a peak of similar intensity suggesting that no metal sintering takes place under reaction conditions. Nevertheless, a shift to a lower 2 $\theta$  value of 39° is observed, ascribed by some authors to a metal phase change through the formation of a Pd-C solid solution, after the use of Pd/C catalysts in similar reactions [27].

### **3.2. Activity and selectivity of PdCCl-1 catalyst.**

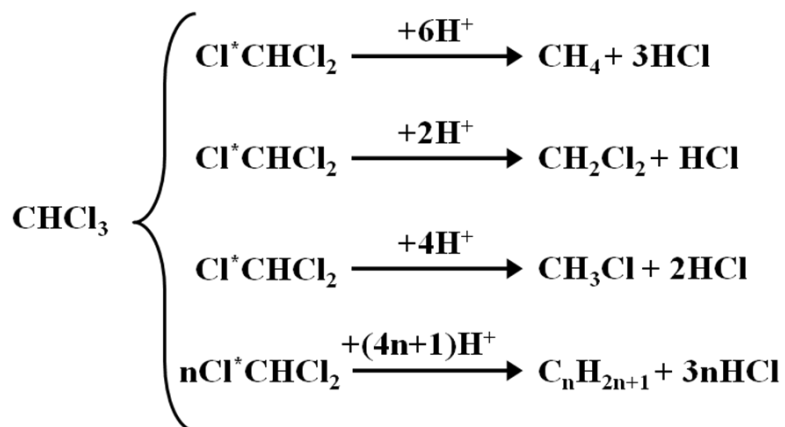
#### **3.2.1. Influence of the reaction temperature and space-time.**

Figure 5 shows the evolution of monochloromethane conversion with the space-time at different reaction temperatures. As can be seen, MCM conversion increases with temperature in the range explored (150-250 °C). Conversion significantly increases with space-time, although the effect becomes less pronounced beyond a space-time around 0.7 kg.h.mol<sup>-1</sup>, especially at temperatures below 200 °C. Methane was the only reaction product and condensation products were not detected. Increasing the temperature up to 250 °C significantly increases MCM conversion, although no more than 35% was reached at the most.

The evolution of dichloromethane conversion with space-time at different reaction temperatures is depicted in Figure 6. Substantially higher conversion values than for MCM were obtained and the increase of conversion with space-time and temperature was more accused. As in the case of MCM, the increase of conversion with space-time becomes less pronounced beyond a space-time value around 0.7 kg.h.mol<sup>-1</sup>. At the highest space-time and temperature tested 93% conversion was reached. The results on product distribution are summarized in Table 2. Methane is by far the main reaction product. The selectivity to monochloromethane decreases as the temperature increases, being lower than 10% beyond 200 °C. Small amounts of ethane and propane were also obtained. As can be observed, the temperature has a significant influence in the product distribution, while the effect of space time is much less important. Selectivity to condensation products (chiefly ethane with very low amounts of propane) is favoured by increasing the temperature, in detriment of methane and MCM.

Figure 7 shows the evolution of chloroform conversion with space time at three different temperatures. As expected, chloroform is by far the more reactive of the chloromethanes investigated. As it is known, the reactivity of chloromethanes decreases as the chlorine content diminishes [15]. Conversion values near 100% were obtained

with a space time of  $0.4 \text{ kg.h.mol}^{-1}$  at temperatures of 150 and 175 °C, conversion greatly increasing with space-time below the aforementioned value. When the temperature was lowered to 125 °C a conversion value around 70% was obtained at that space time which greatly increases up to almost 100% at  $0.6 \text{ kg.h.mol}^{-1}$ . Opposite to the observed for monochloromethane and dichloromethane, a wide diversity of reaction products were obtained from chloroform HDC (Table 3). It is important to note that the selectivity to non-chlorinated compounds was very high, always well above 90%. Methane was again the main reaction product but now close percentages of ethane were obtained together with significant amounts of propane and even butane. Small quantities of ethylene and propylene were also found at the lower space-times. As with DCM, space-time shows no significant effect in product distribution while it is more influenced by temperature. Table 4 compares the selectivities to the different reaction products at the same CLF conversion ( $\approx 70\%$ ) and different temperatures. As can be seen, the selectivity to condensation products (mainly  $\text{C}_2$  and  $\text{C}_3$  hydrocarbons) increases when increasing the reaction temperature, in detriment of methane and dichloromethane. When analysing the evolution of the products yield values with space time (Fig 8a), it can be observed that all the species have a finite rate of formation from chloroform at zero space-time, which indicates that all are primary products formed from chloroform-derived chloride radical. In accordance, the selectivities to all the products present non- zero intercepts when extrapolating to zero space-time (Figure 8b). As stated in previous works (1,26,28), the HDC reaction proceeds through the dissociative adsorption of both, the corresponding chloromethane and  $\text{H}_2$  on the catalyst surface. Thus, the following reaction scheme can be postulated:



Methane, monochloromethane and dichloromethane would be formed from the hydrogenation of the adsorbed dichloromethane radical, while condensation products proceed from the reaction of two or more adsorbed radicals and hydrogen.

The selectivities to monochloromethane and dichloromethane are roughly constant within the wide range of space-time tested (Figure 8b), confirming that methane is exclusively produced from chloroform, through a concerted mechanism, which formally implies the substitution of the three Cl atoms by three H atoms in a single step process, as proposed in a previous work for carbon tetrachloride hydrodechlorination [28]. The concerted mechanism has been proposed to be rather a true consecutive process that takes place in the adsorbed phase on the same active center, *via* a “*rake-type*” mechanism [29-32], in which the intermediate species remain adsorbed. Thus, the extremely fast and stepwise substitution of Cl atoms, from the Cl-surface complexes, by H atoms from  $^*\text{H}$ , proceeds until the adsorbed precursor of methane ( $^*\text{CH}_4$ ) is formed, which desorbs as the stable final product of this surface sequential path while the stoichiometric amount of HCl is produced. It should be kept in mind that this sequence, in the *rake-type* mechanism, does not involve any real physical translation of the surface species. It merely represents the progressive change that the intermediate adsorbed complex undergoes evolving along the reaction coordinate, from  $\text{Cl}^* \text{CHCl}_2$  to  $^*\text{CH}_4$ , on the same active site. Thus, this mechanism is able to explain how methane appears as a primary product from  $\text{CHCl}_3$ , in spite of the fact that transformation of three C-Cl bonds into three C-H bonds is involved.

The overall selectivity to condensation products in general decreases somewhat as the space-time increases. In recent works devoted to the study of the nature and role of the Pd active centers in this reaction [1,26], we experimentally found that they are dual in nature and constituted by the association of neighbouring metallic and electron deficient palladium species:  $[Pd^0 + Pd^{n+}]$ . Hydrogen chemisorbs and homolytically dissociates on  $Pd^0$  to give the adatom Pd-H ( $^*H$ ), whereas the chloromethane chemisorbs on a single  $Pd^{n+}$  site. The formation of the condensation products implies the reaction of two adsorbed chloride radicals, so that the lower concentration of reactant at higher space-times leads to a greater difficulty of finding an adsorbed reactant in the vicinity, leading to a decrease of condensation products selectivity. Correspondingly, the higher proportion of hydrogen relative to the chloride reactant adsorbed, results in a slight increase of methane selectivity as the space-time increases.

### 3.2.2. Comparison among the three chloromethanes.

Figure 9a shows a comparison of the conversion values obtained with the different chloromethanes at a space-time of  $0.08 \text{ kg.h.mol}^{-1}$  and temperatures in the range of 150-250 °C. Similar trends were observed for the other space-time values tested. On the other hand, Figure 9b shows a comparison of the selectivities obtained with the different reactants at the above space-time and a temperature of 250 °C. As stated before, the reactivity highly increases with the chlorine content of the molecule, following the sequence  $CHCl_3 > CH_2Cl_2 > CH_3Cl$ . On the other hand, the selectivity to methane highly diminishes when increasing the chlorine content, being maximum in MCM hydrodechlorination where it is the only reaction product. The low selectivity to methane observed in the HDC of chloroform is not a consequence of a high selectivity to chlorinated products but a high selectivity to non-chlorinated hydrocarbons up to four carbon atoms. The overall selectivity to chlorinated products is slightly lower in the HDC of chloroform than in the case of DCM, although both, dichloromethane and

monochloromethane, are obtained from the former. It can be attributed to the lower reactivity of DCM which may hinder its complete dehalogenation and condensation.

The fact that methane was the only reaction product in the hydrodechlorination of monochloromethane is another evidence of the formation of condensation products through the intermediate hydrocarbon chloride radicals. The dissociative adsorption of monochloromethane leads to the non-chlorinated intermediate  $\text{CH}_3\cdot$ , which appears to present scarce reactivity. The increase in the number of condensation products obtained as the number of chlorine atoms of the reactant molecule increases is consistent with the reaction scheme proposed before, as the reactivity of the molecule increases with the chlorine content [15].

### ***3.3. Influence of the Pd precursor.***

When  $\text{Pd}(\text{NO}_3)_2$  was used as Pd precursor instead of  $\text{PdCl}_2$ , the conversion values decreased (Table 5) for the three chloromethanes investigated. It can be partially attributed to the lower Pd dispersion of PdCN catalyst (Table 1). However, this is not the only cause as the activity per atom of Pd exposed (TOF) was also significantly lower (Table 5). Differences in the nature of Pd were evidenced by XPS (Figures 1 and 2). The catalyst prepared from  $\text{Pd}(\text{NO}_3)_2$  exhibits a lower proportion of electrode deficient Pd which appears to be of significance on the activity of the catalysts. The effect of the Pd precursor is more pronounced in the HDC of dichloromethane (Table 5). In the same way, the Pd precursor also affects to the selectivity patterns of DCM and CLF hydrodechlorination, whereas in the case of monochloromethane, methane is the only reaction product obtained with both catalysts. Selectivity to methane increases when using  $\text{Pd}(\text{NO}_3)_2$  as precursor, in detriment of hydrocarbons with two or more carbon atoms, the effect being more pronounced in the case of chloroform. This confirms that electrode deficient Pd species are involved in the formation of condensation reaction products. From the mechanism proposed before, as the chloromethane is



adsorbed in electrode deficient Pd, reaction of the species adsorbed in two or more of these sites are necessary for the formation of hydrocarbons of more than one carbon atoms, while the amount of  $\text{Pd}^{n+}$  is greatly decreased in PdCN catalyst (Figure 2). On the opposite, the Pd precursor shows a scarce influence in the selectivity to chlorinated compounds. In the case of chloroform, selectivity to monochloromethane and dichloromethane was slightly reduced, while in the HDC of dichloromethane the selectivity to monochloromethane was slightly higher when  $\text{Pd}(\text{NO}_3)_2$  was used as Pd precursor.

### ***3.4. Effect of the particle size of the activated carbon support.***

Table 6 shows the results obtained at different reaction conditions with the catalysts prepared by impregnation of carbon particles of different sizes using  $\text{PdCl}_2$  as precursor. As can be seen, small differences were found in the activity values ( $-r_A$ ), though a slight decrease is observed as the carbon particle size increases. This is in agreement with the very small differences found in Pd dispersion between these catalysts. When the activity per atom of exposed Pd is analysed (TOF), a low although monotonical decrease of activity is also observed as the carbon particle size increases. This is also in agreement with the slight variations in the proportion of Pd species observed by XPS (Figure 3). No significant differences in the selectivity patterns were observed, similar values to those of PdCCl-1 (Table 6) being found for the rest of the catalysts.

### ***3.5. Catalyst deactivation***

Figure 10 shows the evolution of the conversion of the three chloromethanes upon time on stream in long-term experiments with the PdCCl-1 catalyst. Space time and temperature of  $0.24 \text{ kg.h.mol}^{-1}$  and  $150^\circ\text{C}$ , respectively, were used in the case of CLF and  $1.73 \text{ kg.h.mol}^{-1}$  and  $250^\circ\text{C}$  for MCM and DCM. A loss of activity is observed

in all the cases although significantly less pronounced in the case of chloroform. As discussed before, no significant constriction of the porous structure occurred under the operating conditions of the experiments (see Table 1). CO chemisorption results showed a significant decrease in the amount of accessible Pd after the catalyst was used in the hydrodechlorination of DCM. Pd dispersion was reduced from 38% to 9% after 100 h of operation (Table 1). Looking at the DRX profiles of the catalysts (Figure 4), this reduction is not likely to be due to the sintering of Pd particles as no differences in size were found between the fresh and used catalyst. The analysis of the XPS spectra of the used PdCCl-1 catalyst showed a decrease in the proportion of the electro-deficient species of Pd (Figure 1). Considering that the dissociative adsorption of chloromethane takes place on that Pd species, deactivation can be mainly attributed to the poisoning of the active centers with reactant and/or reaction products, which cause a reduction of the accessible metal surface. Deposition of hydrocarbons does not appear to be the cause because in that case it would be expected that the greater deactivation took place in the hydrodechlorination of chloroform as it leads to much higher amounts of hydrocarbon products. On the other hand, the fact that deactivation of the catalyst is more pronounced in the HDC of dichloromethane suggests that poisoning with chlorinated species takes place. The intermediate reactivity of DCM can explain its higher poisoning effect. The high reactivity of chloroform favours its hydrogenation and reaction to condensation products so anyway inhibiting the irreversible chemisorption. The lower reactivity of monochloromethane suggests a lower chemisorption while DCM must be more strongly chemisorbed than MCM but not as reactive as to give rise to a wide diversity of hydrocarbon products upon reaction with other adsorbed radicals, as is the case of CLF.

Very scarce studies of deactivation of supported metal catalysts in the hydrodechlorination of chloromethanes can be found so far in the literature. However several works dealing with the hydrodechlorination of different compounds propose as

one of the main causes of deactivation of these catalyst the formation of carbonaceous deposits, including chlorine in their composition in many cases (27,33,34).

Table 7 shows the evolution of the products distribution upon time on stream. As can be observed, in general the selectivity values do not show significant variations at increasing time on stream. Methane and chloromethanes selectivities (these latter in chloroform HDC) slightly increase with time on stream while those of condensation products slightly decrease. This is consistent with the causes of deactivation discussed before. The poisoning of electrodefficient Pd active sites where the chloromethanes are adsorbed leads to a decrease of these species close to each other thus reducing the possibility of reacting.

#### 4. CONCLUSIONS

Pd on activated carbon catalysts have been prepared showing fairly active in the deep gas-phase hydrodechlorination of monochloromethane, dichloromethane and chloroform, the reactivity following the order  $\text{CHCl}_3 > \text{CH}_2\text{Cl}_2 > \text{CH}_3\text{Cl}$ . High selectivities to non-chlorinated compounds were found (>90% in most cases). Methane is the only reaction product obtained in the HDC of monochloromethane while the diversity of reaction products increases when increasing the chlorine content of the molecule, through the formation of hydrocarbons up to four carbon atoms. The analysis of the evolution of yield and selectivities to reaction products with space-time in the HDC of chloroform with the catalyst prepared from  $\text{PdCl}_2$  and a particle size in the range  $d_p = 0.25\text{-}0.5$  mm, suggests that all are primary products.  $\text{CH}_4$ ,  $\text{CH}_3\text{Cl}$  and  $\text{CH}_2\text{Cl}_2$  come from the hydrogenation of the corresponding adsorbed chloride radical, while hydrocarbons of more than one carbon atoms are formed by reaction and subsequent hydrodechlorination of two radicals adsorbed in neighbouring active centers. The catalyst undergoes a significant deactivation in the HDC of MCM and DCM, specially for this second, whereas it shows much more stable in the case of CLF. It appears to be due to a great decrease of the accessible metal surface which can be

attributed to the poisoning of active centers with chlorinated reactants and reaction products. The use of  $\text{Pd}(\text{NO}_3)_2$  as Pd precursor leads to a decrease in the total activity and TOF of the catalyst due to its poorer Pd dispersion and a lower proportion of electrode deficient Pd species. The use of a different carbon particle size in the preparation of the catalysts does not show a significant effect in the reactivity, at least within the range investigated (0.25-2.8 mm).

## ACKNOWLEDGMENTS

The authors gratefully acknowledge financial support from the Spanish MEC through the project CTQ2005-07579. M.A. Álvarez Montero also wishes to thank the Spanish MEC for her research grant.

## References

- [1] Z.M. de Pedro, L.M. Gómez-Sainero, E. González-Serrano, J.J. Rodríguez, *Ind. Eng. Chem. Res.* 45 (2006) 7760-7766.
- [2] E.D. Goldberg, *Sci. Total Environ.* 100 (1991) 17-28.
- [3] M. Tancredo, R. Wilson, L. Zeise and E.A.C. Crouch, *Atmos. Environ.* 21 (1987) 2187-2205.
- [4] W.J. Hayes, Jr. Laws, Edward R., Jr ; Editors. *Handbook of Pesticide Toxicology, Vol 1: General principles.* Academic press, San Diego (1991), p 497.
- [5] S.Ordóñez, H. Sastre, V.F. Díez, *Appl. Catal. B* 25 (2000) 49-58.;
- [6] M. Legawiec-Jarzyna, A. Srebowata, W. Juszczak, Z. Karpinski, *React. Kinet. Catal. Lett., Vol. 87, No 2, (2006) 291-296.*
- [7] H.M. Chiang, J.W. Bozzelli, *Combust. Fundam. Appl., Jt. Tech. Meet., Cent. East. States Sect. Combust. Inst. (1993) 322-324.*
- [8] A.H. Weiss, S. Gambhir, R.B. Leon, *J. Catal.* 22 (1971) 245.
- [9] A.H. Weiss, S. Valinski, G.V. Antoshin, *J. Catal.* 74 (1982) 136.

- [10] S.Y. Kim, H.C. Choi, O.B. Yang, K.H. Lee, Y.G. Kim, *J. Chem. Soc.: Chem. Commun.* 21 (1995) 2169.
- [11] H.C. Choi, S.H. Choi, Y.G. Kim, O.B. Yang, K.H. Lee, J.S. Lee, *J. Catal.* 161 (1996) 790.
- [12] H.C. Choi, S.H. Choi, K.H. Lee, J.S. Lee, Y.G. Kim, *J. Catal.* 166 (1997) 284.
- [13] E.S. Lokteva, V.I. Simagina, E.V. Golubina, V.V. Lunin, *Kinet.Catal.* 41 (2000) 776.
- [14] B. Aristazabal, C.A. González, A. Barrio, M. Montes, C. Montes de Correa, *J. Molec. Catal. A* 222 (2004) 189.
- [15] T. Mori, K. Hirose, T. Kikuchi, J. Kubo, Y. Morikawa, *J. Japan Petroleum Institute* 45 (2002) 256.
- [16] E. López, S. Ordoñez, H. Sastre, F.V. Díez, *J. Hazard. Mater.* 97 (2003) 281.
- [17] L. Prati, M. Rossi, *Appl. Catal. B* 23 (1999) 135.
- [18] A. Malinowski, D. Łomot, Z. Karpiński, *Appl. Catal. B* 19 (1998) L79-L86.
- [19] T. Mori, T. Kikuchi, J. Kubo, Y. Morikawa, *Chem. Lett.* (2001) 936.
- [20] C.D. Wagner, L.E. Davis, M.V. Zeller, J.A Taylor, R.H. Raymond, L.H. Gale, *Surf. Interf. Anal.* 13 (1981) 211.
- [21] S.H. Ali, J.G. Goodwin, Jr.; *J. Catal.* 176 (1998) 3-13.
- [22] M. Mahata, V. Vishwanathan, *Catal. Today* 49 (1999) 65-69.
- [23] S. Somboonthanakij, O. Mekasuwandumrong, J. Panpranot, T. Nimmanwudtipong, R. Strobel, S.E. Pratsinis, P. Praserthdam, *Catal. Lett.* 119 (2007) 346-352.
- [24] J.L. Gasser-Ramírez, B.C. Dunn, D.W. Ramírez, E.P. Fillerup, G.C. Turpin, Y. Shi, R.D. Ernst, R.J. Pugmire, E.M. Eyring, K.A. Pettigrew, D.R. Rolison, J.M. Harris, *J.non-Crystalline Sol.* 354 (2008) 5509-5514.
- [25] P.A. Simonov, E.M. Moroz, A.L. Chuvilin, V.N. Kolomiichuk, A.I. Boronin, V.A. Likholobov, *Stud. Surf. Sci. Catal.* 91 (1995) 977-987.

- [26] L.M. Gómez-Sainero, X.L. Seoane, J.L.G. Fierro and A. Arcoya, *J. Catal.* 209 (2000) 279-288.
- [27] S. Ordóñez, F.V. Díez, H. Sastre, *Appl. Catal. B* 31 (2001) 113.
- [28] L.M. Gómez-Sainero, X.L. Seoane and A. Arcoya, *Appl. Catal. B* 53 (2004) 101-110.
- [29] J. M., Thomas and W. J. Thomas, Introduction to the Principles of Heterogeneous Catalysts, Academic Press, New York, 1969, Chap. 7.
- [30] X. L. Seoane, P. Boutry and R. Montarnal, *J. Catal.* 63 (1980) 191.
- [31] E. G. Derouane, in F. Ramôa-Ribeiro, A. E. Rodrigues, L. Deane Rollmann and C. Naccache (Eds.), Zeolites: Science and Technology, Martinus Nijhoff Publ., The Hague, 1984. p. 515.
- [32] G. Centi, in R. W. Joyner and R. A. van Santen (Eds.), Elementary Reaction Steps in Heterogeneous Catalysis, Kluwer Academic Publ., Dordrecht, The Netherlands, 1993, p. 93.
- [33] T. Mori, T. Yasuokua , Y. Morikawa, *Catal. Today* 88 (2004) 111.
- [34] C. Concibido, T. Okuda, W. Nishijima, M. Okada, *Appl. Catal. B.* 71 (2007) 64.

## Figure Captions

Fig.1. Pd 3d core level XPS spectra of PdCCl-1 catalyst: (a) as prepared; (b) after reduction in H<sub>2</sub> at 250 °C; (c) after used in HDC of DCM.

Fig.2. Pd 3d core level XPS spectra of PdCN catalyst: (a) as prepared; (b) after reduction in H<sub>2</sub> at 250 °C.

Fig.3. Pd 3d core level XPS spectra of Pd/C catalysts prepared from different activated carbon particle size: (a) as prepared; (b) after reduction in H<sub>2</sub> at 250 °C.

(1) PdCCl-1; (2) PdCCl-2; (3) PdCCl-3; (4) PdCCl-4.

Fig.4. XRD patterns of PdCCl-1 catalyst: (a) after reduction in H<sub>2</sub> at 250 °C; (b) after used in HDC of DCM.

Fig.5. Effect of space-time in the HDC of MCM with PdCCl-1 catalyst at different temperatures: (■) 150 °C; (○) 175 °C; (▲) 200 °C; (Δ) 225 °C; (●) 250 °C.

Fig.6. Effect of space-time in the HDC of DCM with PdCCl-1 catalyst at different temperatures: (■) 150 °C; (○) 175 °C; (▲) 200 °C; (Δ) 225 °C; (●) 250 °C.

Fig.7. Effect of space-time in the HDC of CLF with PdCCl-1 catalyst at different temperatures: (□) 125 °C; (■) 150 °C; (○) 175 °C.

Fig.8. Effect of space-time in the yield (a) and selectivity (b) to reaction products in the HDC of CLF with PdCCl-1 catalyst: (▲) CH<sub>4</sub>; (Δ) C<sub>2</sub>H<sub>6</sub>; (○) C<sub>3</sub>H<sub>8</sub>; (□) C<sub>4</sub>H<sub>10</sub>; (×) MCM; (●) DCM.

Fig.9. Activity (a) and products distribution (b) in the HDC of chloromethanes with PdCCl-1 catalyst: (■) CLF; (Δ) DCM; (●) MCM.

Fig.10. Evolution of chloromethanes conversion upon time on stream with the PdCCl-1 catalyst: (■) CLF; (Δ) DCM; (●) MCM.

### Table Captions

Table 1. Pd content, porous structure and Pd dispersion of Pd/C catalysts.

Table 2. Products distribution in the HDC of DCM with PdCCl-1 catalyst.

Table 3. Products distribution in the HDC of chloroform with PdCCl-1 catalyst.

Table 4. Selectivity to reaction products in the HDC of chloroform at iso-conversion of 70%.

Table 5. Influence of the Pd precursor in the reactivity of the catalyst.

Table 6. Influence of carbon particle size in the reactivity of chloride catalysts.

Table 7. Evolution of selectivity with time on stream.



Table 1. Pd content, porous structure and Pd dispersion of the catalysts.

<b>Catalyst</b>	<b>Palladium content (%)</b>	<b>S<sub>BET</sub> (m<sup>2</sup>/g)</b>	<b>Pore volume (cm<sup>3</sup>/g)</b>	<b>D (%)</b>
PdCCl-1	0.68	1236	0.52	38.1
PdCCl-2	0.82	1255	0.49	35.8
PdCCl-3	0.88	1277	0.49	35.4
PdCCl-4	0.72	1256	0.5	34.7
PdCN	0.81	1255	0.49	26.1
PdCCl-1 used*	--	1282	0.57	9.4

\* In HDC of DCM, after 100 h time on stream.

Table 2. Products distribution in the HDC of DCM with PdCCl-1 catalyst.

$\tau$ (kg.h.mol <sup>-1</sup> )	T (°C)	Selectivity (%)				$\tau$ (kg.h.mol <sup>-1</sup> )	T (°C)	Selectivity (%)			
		CH <sub>4</sub>	C <sub>2</sub> H <sub>6</sub>	C <sub>3</sub> H <sub>8</sub>	CH <sub>3</sub> C I			CH <sub>4</sub>	C <sub>2</sub> H <sub>6</sub>	C <sub>3</sub> H <sub>8</sub>	CH <sub>3</sub> C I
<b>0.08</b>	<b>150</b>	84.35	0.00	0.00	15.65	<b>0.6</b>	<b>150</b>	79.87	3.13	0.00	17.00
	<b>175</b>	77.97	9.43	0.00	12.60		<b>175</b>	78.91	7.51	0.00	13.57
	<b>200</b>	74.48	15.58	0.00	9.94		<b>200</b>	75.78	12.76	0.67	10.80
	<b>225</b>	68.03	22.31	1.65	8.00		<b>225</b>	70.47	19.78	1.14	8.61
	<b>250</b>	62.69	27.94	2.21	7.17		<b>250</b>	64.50	26.56	1.61	7.32
<b>0.24</b>	<b>150</b>	81.52	2.92	0.00	15.56	<b>0.8</b>	<b>150</b>	79.57	3.07	0.00	17.37
	<b>175</b>	79.01	8.43	0.00	12.56		<b>175</b>	78.86	7.23	0.00	13.91
	<b>200</b>	75.03	14.01	0.80	10.16		<b>200</b>	75.95	12.39	0.63	11.03
	<b>225</b>	69.48	20.77	1.34	8.41		<b>225</b>	70.91	19.24	1.09	8.77
	<b>250</b>	63.44	27.34	1.91	7.30		<b>250</b>	64.81	26.49	1.58	7.12
<b>0.4</b>	<b>150</b>	79.60	3.45	0.00	16.95	<b>1.73</b>	<b>150</b>	79.34	2.09	0.00	18.57
	<b>175</b>	78.75	7.74	0.00	13.51		<b>175</b>	79.21	5.93	0.00	14.85
	<b>200</b>	75.43	13.10	0.71	10.76		<b>200</b>	77.43	10.41	0.49	11.66
	<b>225</b>	70.00	20.08	1.23	8.69		<b>225</b>	73.60	16.57	0.86	8.97
	<b>250</b>	63.61	27.34	1.76	7.29		<b>250</b>	67.93	23.90	1.34	6.82

Table 3. Products distribution in the HDC of chloroform with PdCCl-1 catalyst.

$\tau$ (kg.h.mol <sup>-1</sup> )	T (°C)	Selectivity (%)							
		CH <sub>4</sub>	C <sub>2</sub> H <sub>6</sub>	C <sub>2</sub> H <sub>4</sub>	C <sub>3</sub> H <sub>8</sub>	C <sub>3</sub> H <sub>6</sub>	C <sub>4</sub> H <sub>10</sub>	CH <sub>2</sub> Cl <sub>2</sub>	CH <sub>3</sub> Cl
0.08	125	44.72	30.73	0.99	13.26	0.0	5.69	3.36	1.26
	150	39.37	33.59	1.14	14.76	0.49	6.57	2.70	1.38
	175	32.73	36.44	1.85	16.18	0.88	7.51	2.95	1.46
0.24	125	48.58	30.09	0.41	11.21	0.00	4.30	4.52	0.88
	150	44.59	33.06	0.43	12.62	0.00	4.98	3.37	0.95
	175	37.21	37.09	0.61	14.45	0.25	5.96	3.26	1.17
0.4	125	48.53	29.99	0.00	10.87	0.00	4.08	5.08	1.45
	150	45.36	32.86	0.00	12.13	0.00	4.64	3.65	1.36
	175	37.77	37.53	0.00	14.47	0.00	5.85	3.51	0.88
0.6	125	52.67	28.35	0.00	8.87	0.00	3.02	4.68	2.41
	150	47.77	32.61	0.00	11.06	0.00	3.93	3.02	1.62
	175	41.42	37.44	0.00	12.87	0.00	4.72	2.45	1.09
0.8	125	50.47	29.64	0.00	10.17	0.00	3.37	4.75	1.24
	150	45.85	33.17	0.00	12.20	0.00	4.67	3.20	0.91
	175	38.24	37.78	0.00	14.45	0.00	5.80	2.85	0.87
1.73	150	49.13	30.95	0.00	11.02	0.00	4.17	3.96	0.77
	175	42.66	34.53	0.00	13.27	0.00	5.29	2.99	1.25

Table 4. Selectivity to reaction products in the HDC of chloroform at iso-conversion of 70%.

T (°C)	$\tau$ (kg.h.mol <sup>-1</sup> )	Selectivity (%)							
		CH <sub>4</sub>	C <sub>2</sub> H <sub>6</sub>	C <sub>2</sub> H <sub>4</sub>	C <sub>3</sub> H <sub>8</sub>	C <sub>3</sub> H <sub>6</sub>	C <sub>4</sub> H <sub>10</sub>	CH <sub>2</sub> Cl <sub>2</sub>	CH <sub>3</sub> Cl
125	0.4	48.53	29.99	0.00	10.87	0.00	4.08	5.08	1.45
150	0.24	44.59	33.06	0.43	12.62	0.00	4.98	3.37	0.95
175	0.08	32.73	36.44	1.85	16.18	0.88	4.51	2.95	1.46

Table 5. Influence of the Pd precursor in the reactivity of the catalyst.

Chloromethane	Catalyst	T (°C)	X (%)	$(-r_A)$ (mol.h <sup>-1</sup> .g <sub>Pd</sub> <sup>-1</sup> )	TOF (h <sup>-1</sup> )	Selectivity (%)				
						CH <sub>4</sub>	C <sub>2</sub> H <sub>6</sub>	C <sub>3</sub> H <sub>8</sub>	CH <sub>3</sub> Cl	CH <sub>2</sub> Cl <sub>2</sub>
MCM	PdCCl-1	150	0.94	4.41.10 <sup>-6</sup>	1.23.10 <sup>-3</sup>	100	0.00	0.00	0.00	0.00
		175	1.66	7.35.10 <sup>-6</sup>	2.05.10 <sup>-3</sup>	100	0.00	0.00	0.00	0.00
		200	2.87	1.32.10 <sup>-5</sup>	3.69.10 <sup>-3</sup>	100	0.00	0.00	0.00	0.00
		225	4.20	1.91.10 <sup>-5</sup>	5.33.10 <sup>-3</sup>	100	0.00	0.00	0.00	0.00
		250	5.67	2.50.10 <sup>-5</sup>	6.97.10 <sup>-3</sup>	100	0.00	0.00	0.00	0.00
	PdCN	150	0.64	1.23.10 <sup>-6</sup>	5.03.10 <sup>-4</sup>	100	0.00	0.00	0.00	0.00
		175	1.11	3.70.10 <sup>-6</sup>	1.51.10 <sup>-3</sup>	100	0.00	0.00	0.00	0.00
		200	1.95	6.17.10 <sup>-6</sup>	2.52.10 <sup>-3</sup>	100	0.00	0.00	0.00	0.00
		225	3.09	9.88.10 <sup>-6</sup>	4.03.10 <sup>-3</sup>	100	0.00	0.00	0.00	0.00
		250	3.31	1.11.10 <sup>-5</sup>	4.53.10 <sup>-3</sup>	100	0.00	0.00	0.00	0.00
DCM	PdCCl-1	150	2.31	1.03.10 <sup>-5</sup>	2.87.10 <sup>-3</sup>	84.35	0.00	0.00	15.65	0.00
		175	6.68	2.94.10 <sup>-5</sup>	8.21.10 <sup>-3</sup>	77.97	9.43	0.00	12.60	0.00
		200	12.16	5.44.10 <sup>-5</sup>	1.52.10 <sup>-2</sup>	74.48	15.58	0.00	9.94	0.00
		225	20.19	9.12.10 <sup>-5</sup>	2.54.10 <sup>-2</sup>	68.03	22.31	1.65	8.00	0.00
		250	28.61	1.29.10 <sup>-4</sup>	3.61.10 <sup>-2</sup>	62.69	27.94	2.21	7.17	0.00
	PdCN	150	1.05	4.94.10 <sup>-6</sup>	2.01.10 <sup>-3</sup>	74.5	0.00	0.00	25.5	0.00
		175	2.55	9.88.10 <sup>-6</sup>	4.03.10 <sup>-3</sup>	74.3	3.3	0.00	22.4	0.00
		200	4.3	1.61.10 <sup>-5</sup>	6.54.10 <sup>-3</sup>	75.7	5.6	0.00	18.6	0.00
		225	6.32	2.35.10 <sup>-5</sup>	9.56.10 <sup>-3</sup>	76.2	8.9	0.00	14.9	0.00
		250	8.32	3.09.10 <sup>-5</sup>	1.26.10 <sup>-2</sup>	74.9	11.1	0.00	12.0	0.00
CLF	PdCCl-1	125	22.08	1.29.10 <sup>-4</sup>	3.61.10 <sup>-2</sup>	44.72	31.72	13.26	6.95	3.36
		150	47.56	2.65.10 <sup>-4</sup>	7.28.10 <sup>-2</sup>	39.37	34.73	15.25	7.95	2.70
		175	68.98	3.24.10 <sup>-4</sup>	9.05.10 <sup>-2</sup>	32.73	38.29	17.06	8.97	2.95
		200	88.53	3.53.10 <sup>-4</sup>	9.83.10 <sup>-2</sup>	27.42	41.88	18.08	9.16	3.46
	PdCN	125	18.08	5.80.10 <sup>-5</sup>	2.37.10 <sup>-2</sup>	59.54	25.39	6.75	5.29	3.03
		150	38.42	1.21.10 <sup>-4</sup>	4.93.10 <sup>-2</sup>	56.72	28.35	7.40	5.45	2.09
		175	58.23	1.85.10 <sup>-4</sup>	7.65.10 <sup>-2</sup>	55.03	30.56	7.78	4.62	2.01
		200	73.29	2.35.10 <sup>-4</sup>	9.63.10 <sup>-2</sup>	53.37	32.56	8.27	3.56	2.25

\* $C_{A0}$  = 1000 ppm<sub>v</sub>; H<sub>2</sub>/DCM molar = 100;  $\tau$  = 0.08 kg<sub>mol</sub><sup>-1</sup>

Table 6. Influence of carbon particle size in the reactivity of the catalysts.

Chloromethane	T (°C)	$\tau$ (kg.h.mol <sup>-1</sup> )	Catalyst	X (%)	(-r <sub>A</sub> ) (mol.h <sup>-1</sup> .g <sub>Pd</sub> <sup>-1</sup> )	TOF (h <sup>-1</sup> )	Selectivity (%)				
							CH <sub>4</sub>	C <sub>2</sub> H <sub>6</sub>	C <sub>3</sub> H <sub>8</sub>	CH <sub>3</sub> Cl	CH <sub>2</sub> Cl <sub>2</sub>
MCM	250	0.4	PdCCl-1	16.5	1.47.10 <sup>-5</sup>	4.09.10 <sup>-3</sup>	100	0.00	0.00	0.00	0.00
			PdCCl-2	17.0	1.14.10 <sup>-5</sup>	3.52.10 <sup>-3</sup>	100	0.00	0.00	0.00	0.00
			PdCCl-3	16.4	1.02.10 <sup>-5</sup>	3.21.10 <sup>-3</sup>	100	0.00	0.00	0.00	0.00
			PdCCl-4	15.3	8.98.10 <sup>-6</sup>	2.89.10 <sup>-3</sup>	100	0.00	0.00	0.00	0.00
DCM	200	0.4	PdCCl-1	33.8	2.90.10 <sup>-5</sup>	8.53.10 <sup>-3</sup>	75.43	13.10	0.71	10.76	0.00
			PdCCl-2	35.9	2.38.10 <sup>-5</sup>	7.47.10 <sup>-3</sup>	76.45	12.66	0.64	10.26	0.00
			PdCCl-3	35.1	2.16.10 <sup>-5</sup>	6.83.10 <sup>-3</sup>	76.14	12.89	0.61	10.36	0.00
			PdCCl-4	32.0	2.04.10 <sup>-5</sup>	6.55.10 <sup>-3</sup>	76.10	12.88	0.64	10.39	0.00
CLF	125	0.08	PdCCl-1	22.1	1.29.10 <sup>-4</sup>	3.60.10 <sup>-2</sup>	44.72	31.72	13.26	6.95	3.36
			PdCCl-2	31.6	1.22.10 <sup>-4</sup>	3.61.10 <sup>-2</sup>	40.69	31.90	14.47	8.39	4.55
			PdCCl-3	31.5	1.07.10 <sup>-4</sup>	3.20.10 <sup>-2</sup>	40.12	32.09	14.8	8.66	4.32
			PdCCl-4	27.4	9.70.10 <sup>-5</sup>	2.96.10 <sup>-2</sup>	40.16	32.07	14.73	8.63	4.41

Table 7. Evolution of selectivity upon time on stream (Experiments of Fig 10)

Starting Chloromethane	Reaction Product	Selectivity (%)		
		$t_{os} = 10 \text{ h}$	$t_{os} = 50 \text{ h}$	$t_{os} = 90 \text{ h}$
CLF	<b>CH<sub>4</sub></b>	48.32	52.60	53.76
	<b>C<sub>2</sub>H<sub>6</sub></b>	32.46	31.29	30.91
	<b>C<sub>2</sub>H<sub>4</sub></b>	0.30	0.0	0.0
	<b>C<sub>3</sub>H<sub>8</sub></b>	10.13	8.64	8.25
	<b>CH<sub>3</sub>Cl</b>	5.74	4.99	4.78
	<b>CH<sub>2</sub>Cl<sub>2</sub></b>	3.06	2.47	2.30
DCM	<b>CH<sub>4</sub></b>	67.94	71.81	71.76
	<b>C<sub>2</sub>H<sub>6</sub></b>	20.3	15.59	15.5
	<b>C<sub>3</sub>H<sub>8</sub></b>	1.6	1.3	1.3
	<b>CH<sub>3</sub>Cl</b>	10.3	11.3	11.5
MCM	<b>CH<sub>4</sub></b>	100	100	100